PERGAMON

European Polymer Journal 35 (1999) 1883–1894

EUROPEAN POLYMER JOURNAL

On the formation of poly(ethyleneoxide)–poly(vinylalcohol) blends

Rachna Mishra, Kalya J. Rao *

Materials Research Center, Indian Institute of Science, Bangalore 560 012, India

Received 20 February 1998; accepted 21 October 1998

Abstract

Poly(ethyleneoxide)–poly(vinylalcohol) blends were prepared and characterized using thermal, spectroscopic and structural methods. By all indications the blends appear to be microscopically inhomogeneous with no strong interpolymer bonding. The high degree of crystallinity in PEO regions induces a significant degree of ordering in neighbouring PVA regions, as evident from thermal properties. PVA obtained from solvent evaporation exhibits an irreversible endothermic transition which could be order–disorder type. Both IR and NMR spectroscopies also suggest the presence of subtle structural ordering influence of PEO on PVA. It is found to be possible to prepare self supporting films of the blends which consists of fine dispersion of PEO and PVA in each other.

1. Introduction

Both poly(ethyleneoxide) (PEO) and poly(vinylalcohol) (PVA) are industrially important polymers and their blends can be of significant practical utility. PEO is a simple chain polymer with etheric linkages while PVA is a polymer with a carbon chain backbone with hydroxy groups attached to methane carbons. These -OH groups can be a source of hydrogen bonding (H-bonding) and hence of assistance in the formation of polymer blends [1–7]. However, most commercial PVA samples are made from hydrolysis of poly(vinylacetates) or PVAc, and as a result about 18% of unhydrolysed acetate groups are retained in the structure attached to the methine (-CH) carbon. The bulky acetate groups randomly distributed on the polymer chain in such samples prevent OH groups on neighbouring chains from getting close enough to form interchain hydrogen bonds, but in spite of this feature, interchain hydrogen bonding in PVA polymer cannot be altogether ignored. The melting point of pure PVA is significantly higher compared to that of PEO of comparable chain length and this feature can be partly attributed to this interchain hydrogen bonding present in PVA. However the more important reason for the higher melting point of PVA could be the higher strength of the C–C–C backbone in PVA compared to that of C–O–C backbone in PEO. The likelihood of strong H-bonding between PEO and PVA is low since the oxygen in PEO is etheric in nature. However formation of weak H-bonds between PEO and PVA cannot be ruled out. The C–O–C bond angle in PEO is normally 108° and when a -OH group from a neighbouring PVA chain approaches the etheric oxygen atom in order to form a H-bond, the C–O–C bond angle deviates from 108° so that the lone pair of the etheric oxygen is positioned nearer to the approaching OH from PVA. It would therefore be interesting to investigate the structure and thermal properties of the

* Corresponding author. Tel.: +91-80-3344411, ext. 2583; fax: +91-80-3311310 or 3341683; e-mail: kjrao@sscu.iisc.ernet.in

0014-3057/99/$ - see front matter
PII: S0014-3057(98)00283-3

composites formed in the PEO–PVA system with different proportions of the components. Such investigations will also be useful in designing electrolytes for battery applications by incorporating ionic salts in the crystalline or glassy state. In this paper we have examined PEO–PVA composites over the entire composition range using thermal, spectroscopic and structural methods. We have found that mutual miscibility of PEO and PVA is likely to exist over only a small range of compositions. The mixtures otherwise seem to form only microscopically immiscible blends which do not possess a tendency for extensive mutual solubility. They are referred to as incompatible polymer blends or simply blends throughout this paper. It is, however, possible to prepare films of good mechanical properties using these incompatible blends of PEO and PVA and this aspect has been examined in this paper.

2. Experimental

2.1. Materials and measurements

PEO and PVA were acquired from commerical sources, Aldrich (USA) and S. D. Fine Chemicals (India), respectively). PVA was reported to contain 18% of unhydrolysed acetate. This value was confirmed from independent chemical analysis for acetate [8], NMR analysis of methyl and methylene protons [9] and C-13 NMR of exchanged acetate groups [10]. Molecular weight of PEO was provided by Aldrich ($=6\times10^5$). Molecular weight of PVA was determined by the viscosity method and was found to be 137,770. Intrinsic viscosity of PVA solution in water (deionized and double distilled) was determined experimentally by measurements of flow times in a standard capillary viscometer. The specific viscosity η_{sp} and concentration C of the polymer were used to make a standard Huggin's plot. The η_{sp}/C values were extrapolated to $C = 0$. The intrinsic viscosity, η_{intr}, was then calculated by using Mark Houwink equation, $\eta_{intr} = KM_v^{\alpha}$ where K and α are empirical constants for the particular system [11]. In order to prepare films of the blends, various mixtures of PEO and PVA were dissolved in a mixture of deionized and distilled water and n-propanol taken in the ratio 1:1. Films were cast with these solutions either on glass slides or on teflon sheets, the latter was found to be advantageous when lifting the films off the supports. The films were first dried in air and then in a vacuum oven at less then 65°C (melting temperature of PEO). It was possible to prepare films of all compositions and these are listed in Table 1 along with the sample codes used in the text for convenience of reference.

Table 1
Decomposition temperature from TGA

Blend (PEO:PVA) compositions (mol%)	Sample code	Temperature, T_1(°C)	Temperature, T_2(°C)
100:0	A	369	–
90:10	B	351	–
80:20	C	351	–
70:30	D	257	354
60:40	E	252	357
50:50	F	244	364
40:60	G	251	366
30:70	H	247	355
20:80	I	247	370
10:90	J	246	377
0:100	K	256	397

2.2. Characterization

X-ray diffraction (XRD) patterns of the films were recorded for the films on a Scintag Inc. (USA) XDS 2000 XRD machine. The films were given a 20 Å sputter coat of gold and were examined in scanning electron microscope (SEM), S360 (Cambridge Instruments, England). Small pieces of the films were cut and loaded into a thermal analyser to obtain both thermogravimetric and differential thermal analysis (DTA 1500, Polymer Laboratory). The rates of heating were so adjusted as to obtain a clear recording of both phase transitions and decompositions. A 5°C/min heating rate was employed and both TGA and DTA were performed in dry nitrogen atmosphere. Infrared spectra of both the blends and the pure components were obtained using the films on an FTIR spectrometer (IFS 113 V, Brucker). Samples were dissolved in perdeuterated dimethylsulphoxide (DMSO-d^6) and ^{1}H NMR spectra were obtained on an AMX 400 MHz NMR spectrometer.

3. Results and discussion

3.1. X-ray diffraction

X-ray diffraction (XRD) patterns of the blends and the pure components are shown in Fig. 1 in the order of decreasing proportion of PEO. It may be seen that pure PVA exhibits only a broad and shallow diffraction feature around the 2θ value of 18°, indicating the presence of low-degree crystalline ordering. PEO has two well-defined reflections at 2θ values 19.1° and 23.3°. These reflections are consistent with literature reports on crystalline PEO [12–14]. It was difficult to make estimates of crystallinity using the XRD data. We have assumed that PEO is about 60% crystalline

based on literature reports on similar preparation from solution evaporation and melt cooling ($\Delta H = 37.26$ cal/g [15]). All the blends show these two reflections and the XRD patterns are reproducible in all the compositions. This unique and unchanging feature in XRD patterns of PEO containing films suggests that PEO and PVA remain as separate phases with no significant mixing. Therefore there seems to be no pronounced inter PEO–PVA hydrogen bonding and they form incompatible PEO–PVA blends in the sense described earlier. It may be noted that thermal cycling of the blends did not affect any of the features in the XRD patterns.

3.2. Thermal studies

Differential thermograms (DTA) for the first (I) heating cycle and the second (II) reheating cycle for various compositions are shown in Fig. 2a and b, respectively. Fig. 2a corresponds to I heating of the film materials up to 220°C. These samples were cooled and reheated [16]. The thermograms corresponding to reheating (II) are given in Fig. 2b. The results of thermogravimetric analysis are presented together in Fig. 3. The present DTA/TGA setup was not sensitive enough to record the glass transition temperatures of the blends, although other thermal events such as melting and decomposition were clearly identified. Pure PEO and two of the PEO rich compositions exhibited single major weight loss event around 400°C. All other compositions registered two events, which occurred around 250°C and around 350°C. The temperatures of these decompositions are given in Table 1 and the manner of determination of these temperatures is illustrated in Fig. 3 for the case of PEO:PVA, 20:80 (intersection of dotted lines) sample code designation, I.

Pure PEO exhibits an endothermic melting transition in DTA. This endotherm appears during the second heating also and with almost equal area under the endothermoic peak. It is therefore implied that PEO is recrystallized upon cooling from the molten state to the same extent as in the starting material. This essentially reproducible extent of crystallinity of PEO is assumed to be 60% as reported in the literature [15].

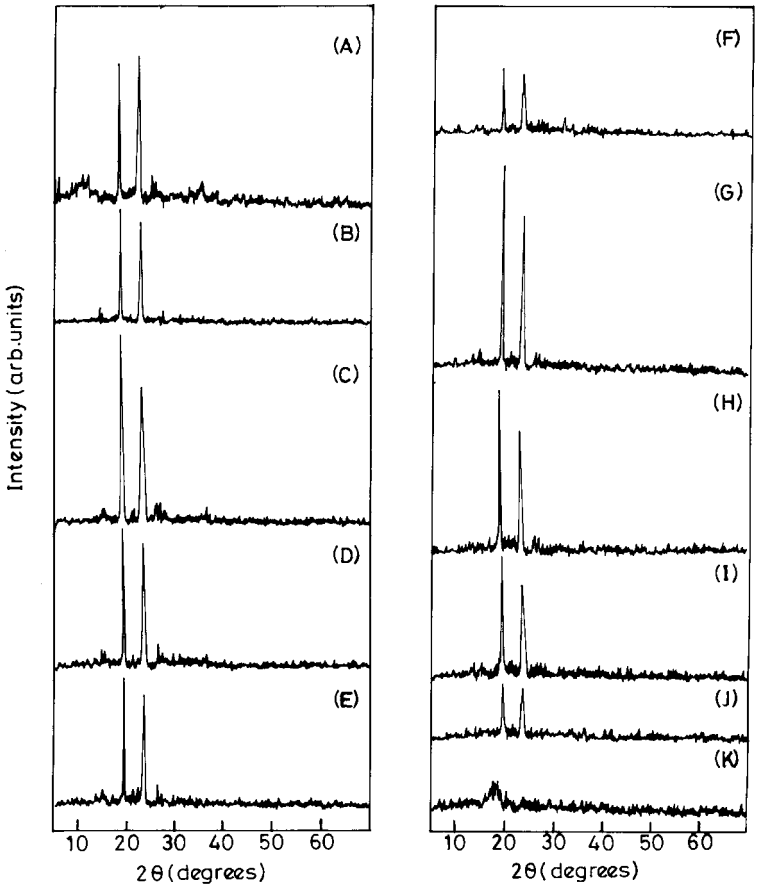

Fig. 1. X-ray diffraction pattern of pure components and blends (description of the sample codes are given in Table 1).

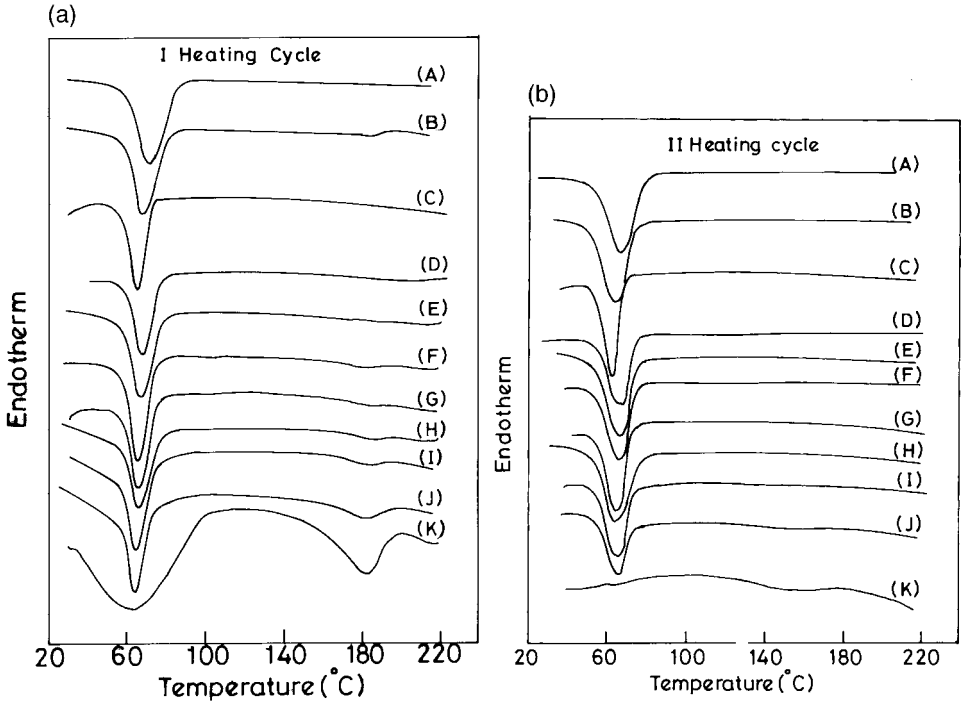

Fig. 2. (a) Differential thermograms for the I heating cycle of pure components and the blends. The letters A, B, C etc. refer to the sample codes given in Table 1. (b) Differential thermograms for the II heating cycle of pure components and the blends. The letters A, B, C etc. refer to the sample codes given in Table 1.

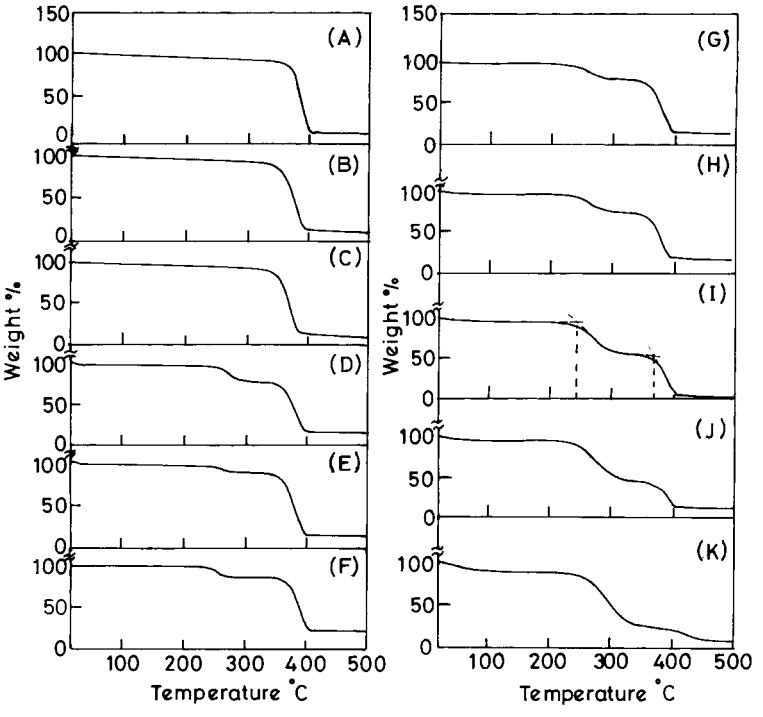

Fig. 3. Thermogravimetric curves of pure components and the blends.

Pure PVA exhibits a fairly large endotherm in DTA around 65.8°C and a melting endotherm at 183°C during the I heating [17]. However in the II heating these endotherms vanish. The endotherm at 65.8°C in I heating cannot be due to escape of trapped solvent because there is no weight loss at this temperature as seen in TGA (Fig. 3). We tentatively attribute this to a disordering phase transition of PVA. PVA develops a low degree of crystallinity when prepared as a film from solution evaporation and it is indicated by the presence of a shallow but definite peak at $2\theta = 18^\circ$ in the XRD (Fig. 1). The first thermal cycling results in complete conversion of PVA into a glass because it was melted and cooled and the XRD of this sample does not possess the 18° shallow peak in XRD. Assuming that in the composites prepared from solution evaporation PVA behave in the same manner as in pure PVA films (do not contribute to the endothermic events during second heating cycle), thermograms in Fig. 2b were analysed for the enthalpy changes. This was accomplished using the known molar heat of melting of PEO and comparing the areas under the melting endotherms of various compositions [18]. It was also assumed that PVA in the samples does not affect the melting characteristics of PEO. The molar enthalpies so determined are listed in Table 2. It is noticed that there is a considerable increase in the enthalpy of melting (up to three times or more) as the proportion of PVA in the blend is increased up to 80 mol%. Above 80% PVA the enthalpy drops rapidly. However the increases are not systematic and the scatter in the values is significant. This may be partly a consequence of a spread in the sizes of the inhomogenous phases or in the degree of crystallinity of PEO formed in the blends after the first thermal cycling. However the interesting aspect is the observation of enhanced enthalpy of transition just above ~60°C, corresponding to the melting point of PEO. We attribute a structural origin to the apparent increase of the enthalpy of melting of PEO crystallites. This increased enthalpy observed at the melting point may not originate from PEO crystallites as such but may be due to its influence on the PVA in the interfacial region. The influence is one of inducing crystalline order in the interfacial region. The disordering transition of the crystalline PVA layers adhering to PEO clusters is responsible for the observed enhanced enthalpy of the above transition. This induced ordering of PVA can be likened to the "rigid amorphous phase" concept of Wunderlich [19]. The ordered region in PVA is metastable in the sense that it exists only in the region interfaced to PEO and gets disordered when PEO itself melts around 60°C. The layers of PVA ordered in this manner by the influence of crystalline PEO behave like adherent cocrystallites of PVA and as they disorder they add their disordering enthalpy to the observed melting enthalpy of PEO and is not stable in the absence of supporting PEO structure. The ordering of PVA in the interfacial region may not be governed by strong chemical interactions between PVA and PEO because the melting temperature of PEO itself remains unaffected.

Table 2
Melting enthalpy of PEO in II heating cycle

Blend (PEO:PVA) composition (mol%)	Enthalpy (cal/g)
100:0	21.8
90:10	29.1
80:20	27.9
70:30	30.2
60:40	38.2
50:50	41.1
40:60	41.1
30:70	65.3
20:80	63.7
10.90	8.3
0:100	0.0

We referred earlier to the observation of an endothermic disordering transition in pure PVA films during I heating (Fig. 2a). The nature of this metastable and weakly crystalline order may not be the same as in the PEO induced ordering in the interfacial layers of PVA in blends. The enthalpy, ΔH of the disordering transitions of adherent PVA cocrystallites in the interfacial regions in the blends has been evaluated in the case of 30% PEO containing sample and found to be about 65 cal/g. However the ΔH of the irreversible disordering transition in pure PVA films prepared from solvent evaporation was much lower and found to be 10.7 cal/g. Therefore the PEO induced crystallinity in PVA is likely to be quite different and also significant.

From Fig. 3 we note that in pure PVA there are two stages of decomposition, whereas in pure PEO there is only one sharp decomposition around 400°C. No effort has been made to confirm the decomposition products as it is well known that the decomposition leads to evolution of lower molecular weight alkanes, alkenes, aldehydes, ketones, etc. and also acetaldehyde and acetic acid in the case of PVA [20–22]. In all compositions the signatures of the two decomposition stages are manifest in the TGA of the films. The temperature of the second decomposition stage of PVA roughly coincides with the temperature of the only decomposition of PEO and therefore the nature of decomposition process at this temperature is quite complex. We have however tried to follow the decomposition kinetics through these two stages using standard methods of

analysis and the data obtained from TGA. For example in Fig. 4a and c we have presented $\Delta \log U$ (along the y axis) versus $\Delta \log W$ (along the x axis) plots of few typical decompositions (method I), where U and W are the rate of decomposition and fractional weight loss, respectively. It is found that the variation is quite linear, suggesting that Freeman and Carroll [23] type of analysis is applicable for the kinetics of these decompositions. It is assumed in such kinetics that the solid decomposes to give another solid and the rate (U) is related to instantaneous weight fraction of the material W by the equation,

$$U = -\mathrm{d}W/\mathrm{d}T = A\exp(-E/RT)\cdot W^n/U_\mathrm{h}$$

where U_h is the heating rate = 5°C/min, A = frequency factor/min, E is the activation energy in cal/gmol, T is the temperature in K, R is the gas constant = 1.987 - cal/deg mol, and n is the order of reaction. The weight fraction W is taken as the ratio of the weight of the material present at time t to the initial weight of the sample (at $t = 0$). TGA data has also been plotted as $\Delta \log U/\Delta \log W$ versus $\Delta\,(1/T)\Delta \log W$ in Fig. 4b and d (method II) where Δ refers to the differences in the corresponding quantities for various time intervals. The linearity of the plots again confirms the validity of Freeman–Carroll kinetics. The activation barriers and the orders of the reaction are also obtained by the above methods. There is good agreement in ΔE and n values obtained by the two methods. The decomposition temperatures T_1 and T_2 corresponding to the data in Table 1 are shown in Fig. 5a and the corresponding activation barriers and n values are given in Table 3 for both low temperature (T_1) and high temperature (T_2) decompositions. The activation barriers shown in parentheses in Table 3 are from method 2. The activation barriers for the high temperature decomposition generally decrease, but the barriers of the low temperature decomposition (present only in PVA containing blends) decrease even more rapidly as the PVA content increases. This is expected because the spread of temperature over which decomposition occurs increases for the low temperature decompositions. In PEO rich films the spread is small and the films exhibit thermal stability over greater range of temperature than in the PVA rich samples. Thus there

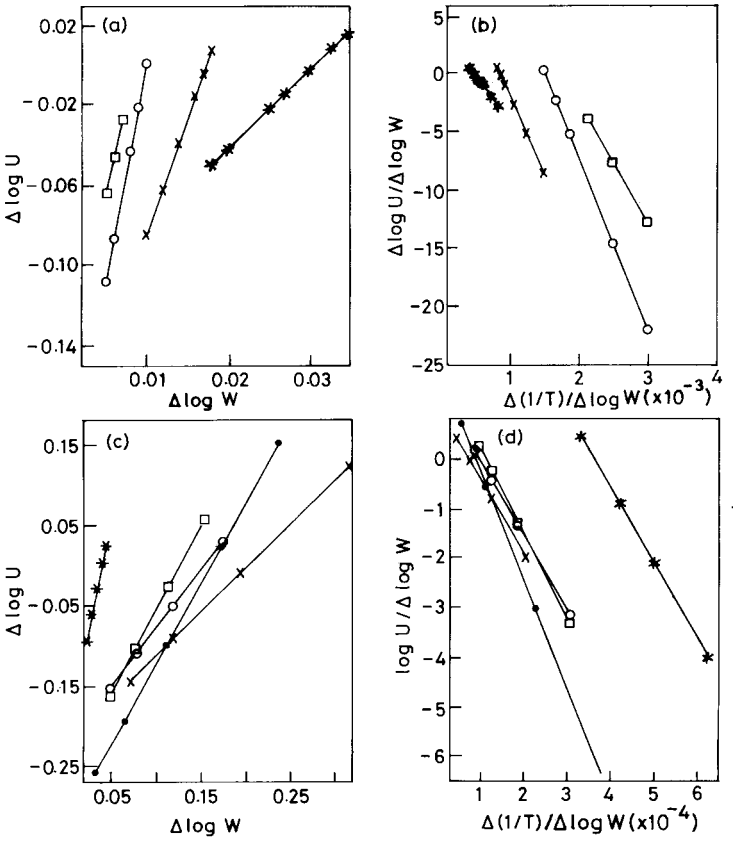

Fig. 4. TGA kinetic plots: at low temperature (a), (b) and at high temperature (c), (d) for samples A (●), B (○), G (□), I (×), (K) (*).

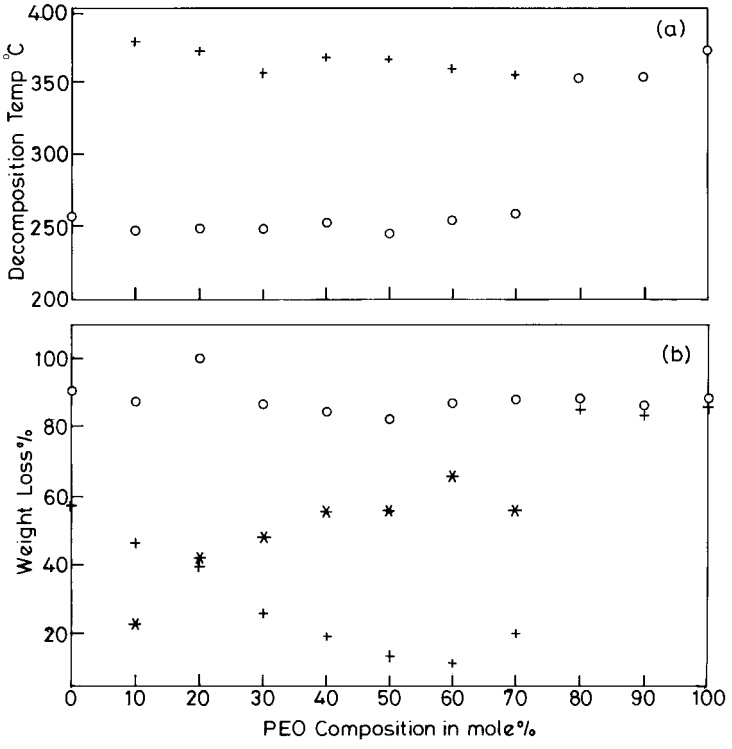

Fig. 5. (a) Decomposition temperature variation with PEO composition: at high temperature (+), and at low temperature (○); (b) total wight loss percentage (○), low temperature weight loss percentage (+), and high temperature weight loss percentage (*) as a function PEO composition.

Table 3
Kinetic parameters for thermal degradation of PEO–PVA blends

Blend composition (mol%)	Low temperature, method 1 (method 2)		High temperature, method 1 (method 2)		Temperature range	Residue (% at 500°C)
PEO:PVA	E_a (kcal/mol)	n	E_a (kcal/mol)	n	(°C)	
100:0	100(100)	2.0	–	–	370–407	11.9
90:10	66(64)	1.8	–	–	351–400	13.8
80:20	70(70)	1.6	–	–	351–400	11.8
70:30	91(90)	–	–	–	257–293	–
	–	–	72(73)	1.9	354–400	12.3
60:40	98(101)	–	–	–	252–287	–
	–	–	68(67)	1.7	357–400	13.3
50:50	136(135)	–	–	–	243–272	–
	–	–	80(79)	2.0	366–406	18.0
40:60	47(47)	–	–	–	251–291	–
	–	–	90(89)	2.4	364–404	16.0
30:70	66(68)	–	–	–	247–295	–
	–	–	67.56(69)	1.4	355–396	13.8
20:80	61(61)	–	–	–	247–295	–
	–	–	67.32(68)	1.1	370–407	–
10:90	53(54)	–	–	–	246–301	–
	–	–	68.5(69)	1.8	377–403	9.8
0:100	37(36)	–	–	–	256–353	–
	–	–	67(68)	–	397–453	9.8

is a significant thermal stabilization in PEO rich blends. The weight loss at the second stage of decomposition increases monotonically as a function of PVA content in the blend (Fig. 5b). The weight loss at the lower temperature increases correspondingly (Fig. 5b). The total weight loss is around 85% in all the compositions and the residual weight is around 15% (see Table 3). A cursory examination of Figs. 3 and 5b also suggests that the blends are essentially mixtures of PVA and PEO and only a moderate interpolymer interaction can be expected to be present. The low and high temperature decomposition kinetics are again suggestive of the absence of strong inter polymer interaction in the mixtures because the two stages clearly correspond to different Freemann–Carroll kinetic parameters. The temperatures of decompositions are affected only mildly (Fig. 5a).

Pure PEO and pure PVA leave residues of about 12% and 10%, respectively, when heated to 500°C. However when the blends are decomposed the residues are generally slightly higher than these values. This may be taken as an indication of the presence of a small extent of mutual solubility of PVA and PEO. In the case of pure PVAc Tsuchiya and Sumi [20] reported the weight of the residue as 52.1%. The PVA used in our experiments contains 18% unhydrolysed acetate groups which makes it effectively a molecular blend of 82% PVA and 18% PVAc. Assuming that the

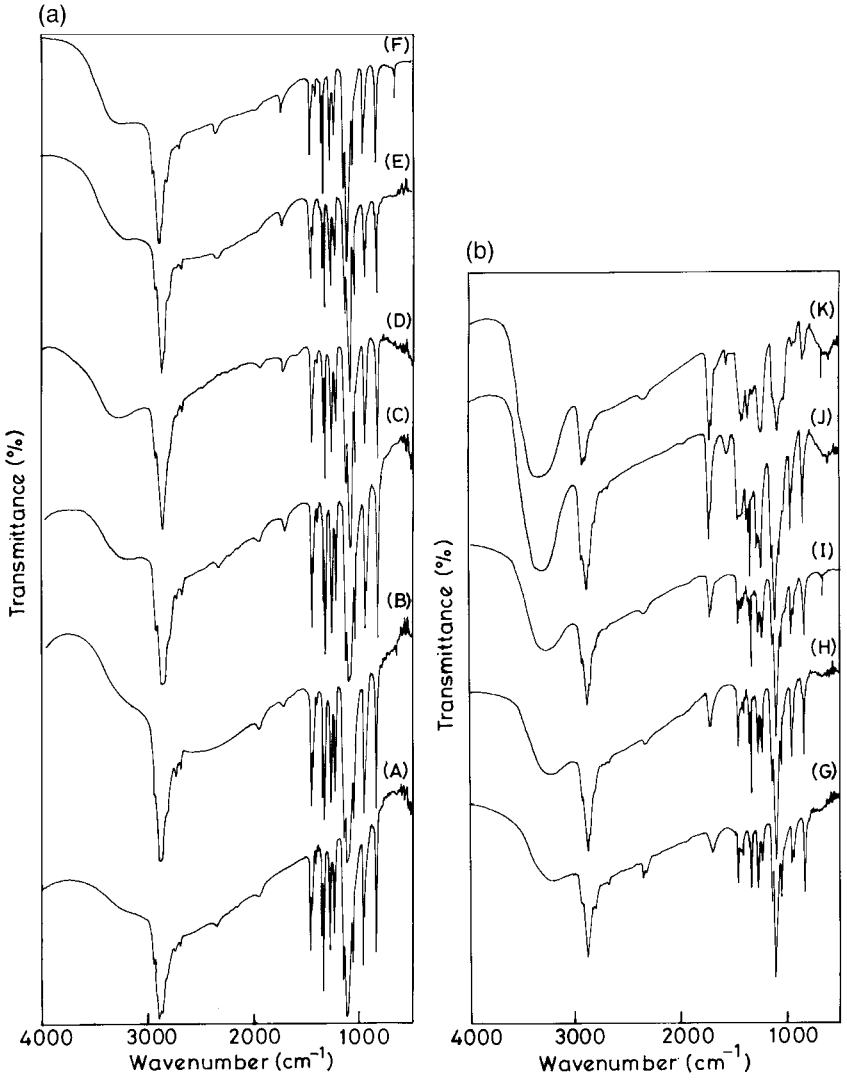

Fig. 6. (a) and (b) FTIR spectra of pure components and blends. (c) FITR absorption intensity calculated by taking area under the peaks as histograms for samples A, D, F, H and K.

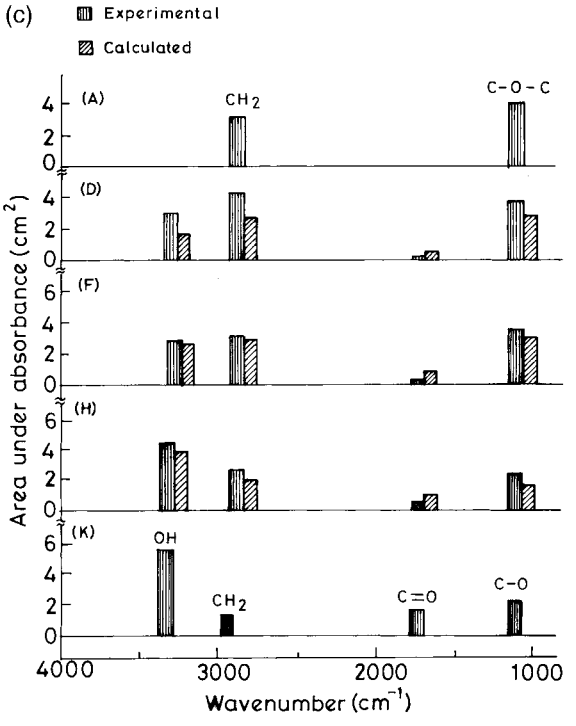

Fig. 6. *continued*

18% PVAc is responsible for the observed residue in PVA we should expect 9.8/0.180 = 54.4% residue in 100% PVAc and this value is in reasonable agreement with the analysis of Tsuchiya and Sumi.

3.3. Spectroscopic studies

The infrared spectra of the blends are presented in Fig. 6a and b. Both PVA and PEO exhibit a number of IR [24,25] absorbtion features below 2000 cm^{-1}. The most important of these appears to be C=O stretching at 1740 cm^{-1}, CH_2 asymmetric bending at 1340 cm^{-1} and COC stretching around 1110 cm^{-1}. Features above 2000 cm^{-1} are both intense and composition sensitive. They are the νCH_2 stretching at 2885 cm^{-1} and a ν_{OH} stretching at 3400 cm^{-1}. Where as ν_{COC} stretching is present only in the spectra of PEO, ν_{OH}, $\nu_{C=O}$ (from the unhydrolysed acetate group of PVA) are present only in the spectra of PVA. The absence of ν_{OH} and $\nu_{C=O}$ is evident in the IR spectra of even PEO rich blends in Fig. 6c and so is the absence of ν_{COC} in PVA rich compositions.

In order to examine the influence of compositions on various IR absorption peaks areas under the respective peaks were measured and a comparison is made [26] in Fig. 6c for three blends and two pure components as histograms of absorption intensity. On the basis of absorption intensities in pure components the expected intensities of absorption of the blends were calculated assuming that the blends are non-interacting mixtures of PVA and PEO polymers. These intensities are juxtaposed in Fig. 6c for the case of blends. It is interesting to note from the Fig. 6c that the absorption due to COC stretching frequencies in the blends is higher than that expected from PEO concentration in the blend. The same trend is observed in ν_{CH_2} and ν_{OH} (while calculating the intensities of CH_2 groups presence of CH_2 groups in both PEO and PVA was both taken into account). The intensities of C=O stretching are lower than their expected values in the blends. However, the frequency of OH vibration itself remains unaffected and therefore intermolecular hydrogen bonding between PVA and PEO may not be of significance at all. Nevertheless the increase of the OH absorption intensity needs to be understood. We note in this context that PEO induces crystallinity of adherent PVA in the interfacial regions of the blends. This process may be responsible for the increase in OH vibrational intensities, because at the interfaces the confirmational geometry of the HC–OH group is so altered that the value of $(d\mu/dr)$ for the vibrational transition is effectively increased (μ and r are the dipole moment and the corresponding coordinate which undergo change during transition [27]). This increases the intensity of the transition. Similarly, the increase in the intensity of COC stretching absorption is also likely to arise from local (interface) confirmational modification in the interfacial region and the consequent change in the value of $(d\mu/dr)$ of the corresponding vibrational transition. The helicity in the crystalline packing of PEO is likely to be altered which causes a decrease in COC angle. This in turn affects the $(d\mu/dr)$ values and hence the absorption intensities. Just the opposite trend is observed in the intensities of C=O stretching frequencies. We can only conjecture that in the adherent crystallite regions of PVA in the blends there is some geometrical restriction which decreases the value of vibrational intensity matrix element of C=O. The IR spectroscopic observations therefore may be considered as confirming the presence of weak interaction between PEO and PVA in the composites which is of the nature of a subtle influence of the PEO which results in the development of crystallinity in interfacial regions of PVA. The IR spectra of thermally cycled samples did not exhibit any noticeable changes.

The influence of PEO in inducing crystallinity in the interfacial region of adherent PVA is even more clearly evident in the ^1H NMR spectra of the blends in comparison to those of the pure components presented (Fig. 7). The resonances have been identified from the assignments made in the literature for PVA [9]. The spectra of PEO [28] is rather simple and consists of a low intensity resonance of CH_2 protons; the CH_2

group is flanked by an etheric oxygen on one side and another CH_2 of similar nature on the other side in the PEO structure. The resonance occurs at a chemical shift value of 3.7 ppm. It is seen that this single weak but sharp, resonance of CH_2 protons disappears in all the blends. The resonances due to methine protons (-CH (V_A)) of PVA also virtually disappear in the blends. These absences in the spectra of blends are indicated by dots in the spectra of the blends. Both the CH_2 protons in acetate diads (V_A, V_A) and two methylene protons (-CH_2) in alcohol diads (V_{OH}, V_{OH}) are unaffected in the spectra of the blends. A weak resonance is observed around 1.2 ppm in PVA and also in PEO poor samples. The intensity of this peak increases in PEO rich samples although it is absent in pure PEO itself which is intriguing. The origin of this resonance is unclear but it is tentatively attributed to the backbone CH_2 protons in the adherent crystalline regions of the PVA.

No attempt is made here to analyse completely the NMR spectral features but what is indicated in NMR is that in the blends of PEO and PVA exhibit subtle structural changes due to some weak intermolecular interactions which is not of the nature of H-bonding.

3.4. Morphological studies

For the practical films it would be essential to know the microstructures of the blends [29, 30]. Scanning electron micrographs (SEM) of selected composition are shown in Fig. 8. SEM of pure PEO and PVA films cast from aqueous solutions exhibit no features attributable to any crystalline morphology. Neither the formation of lamallae nor of the spherulites was noticed. Therefore the crystallinity in PEO and other blends inferred and discussed earlier are likely to be submicroscopic in dimensions. However when films are cast from DMSO solution, formation of PEO crystallites is noticed and the crystallites exhibit microscopic fibrous morphology as shown in Fig. 8b. Blends of PEO:PVA 40:60 (Fig. 8c) and 50:50 (Fig. 9a) cast as films from aqueous solutions exhibit phase separation with droplet like [31] features. These droplets are likely to be amorphous PVA while the other portions which

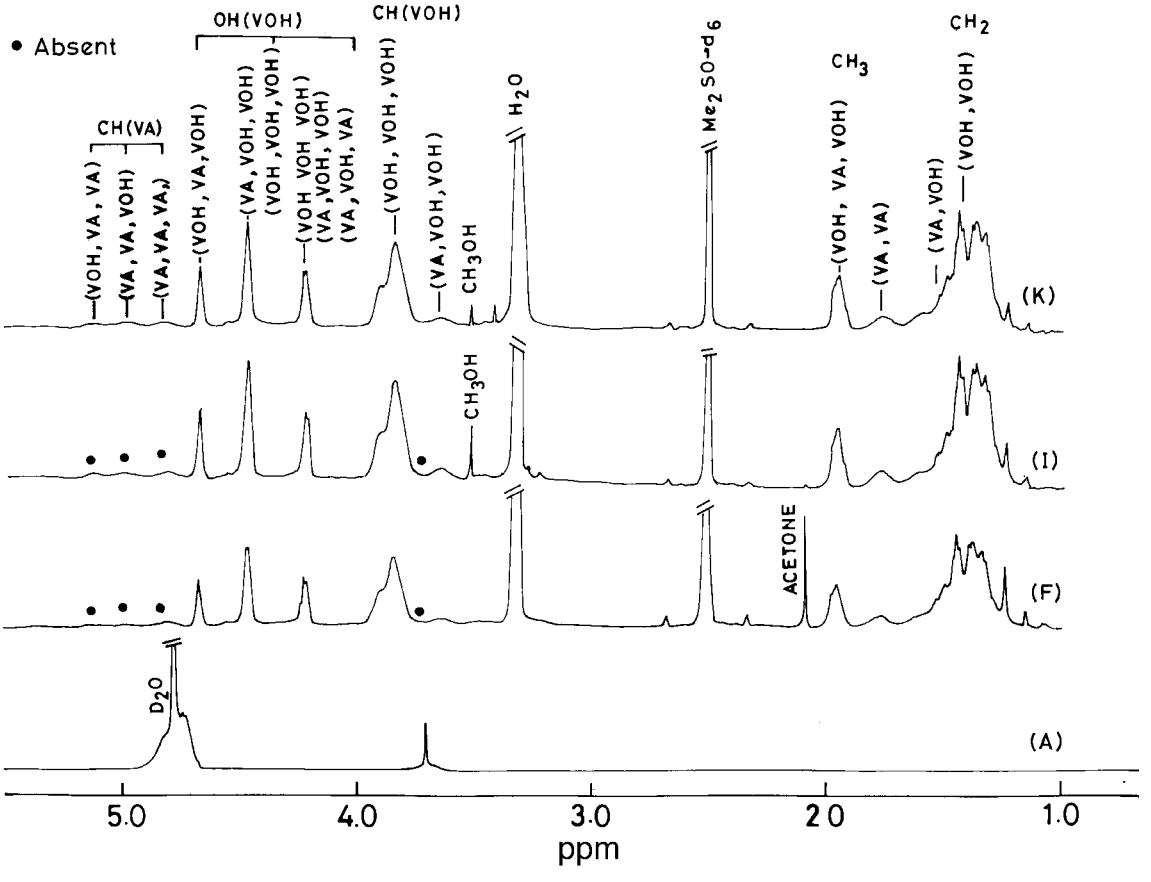

Fig. 7. Proton NMR spectra of samples A, F, I and K.

appear like lamellae are PEO. But in the case of 50:50 blend there was evidence of only the formation of lamellae which are also sparse and distributed in an amorphous matrix. It is difficult to identify features in SEM attributable to induced crystallization of PVA. The SEM micrographs of PVA rich composition (Fig. 9b) are essentially featureless with only occasional feature attributable to the formation of fibroids. Both in PEO rich and PVA rich blends neither the droplet nor the lamellaer morphology were as prevalent as in some intermediate compositions. The microstructure therefore confirm the absence of miscibility of the two polymers in support of earlier discussions.

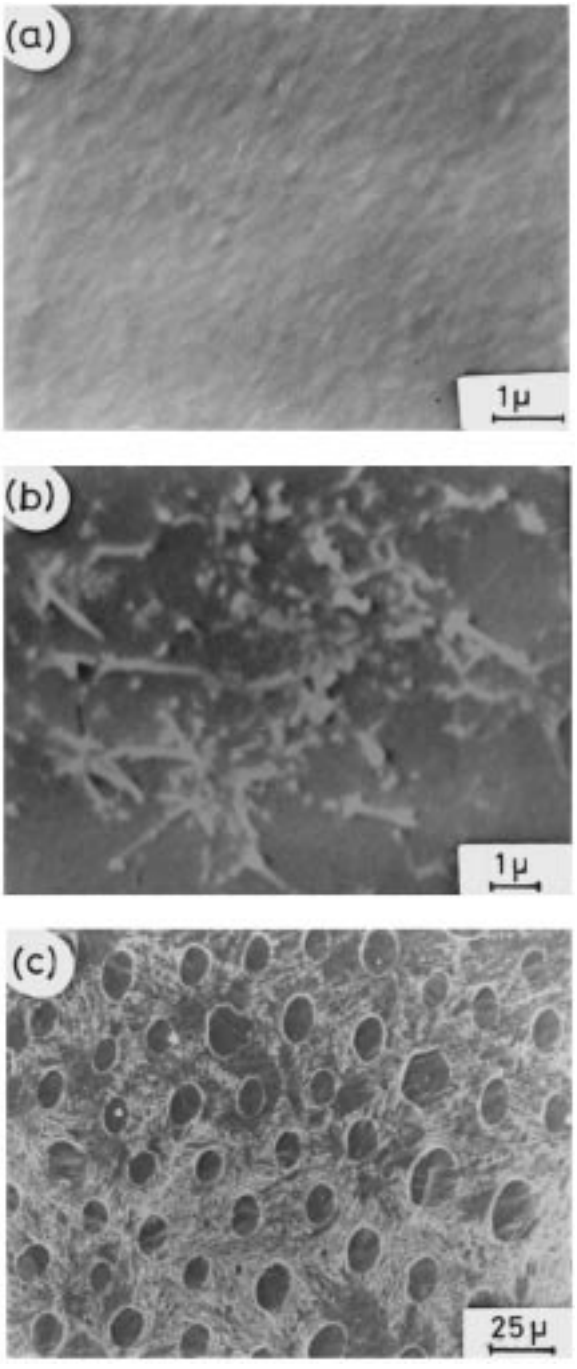

Fig. 8. Scanning electron micrographs of (a) pure PVA cast from aqueous solution; (b) PEO crystallites formation in pure PEO films cast on glass substrate; (c) phase segregation (droplet morphology) for sample (G) where PVA is rimmed and enclosed by PEO fibrous crystallites.

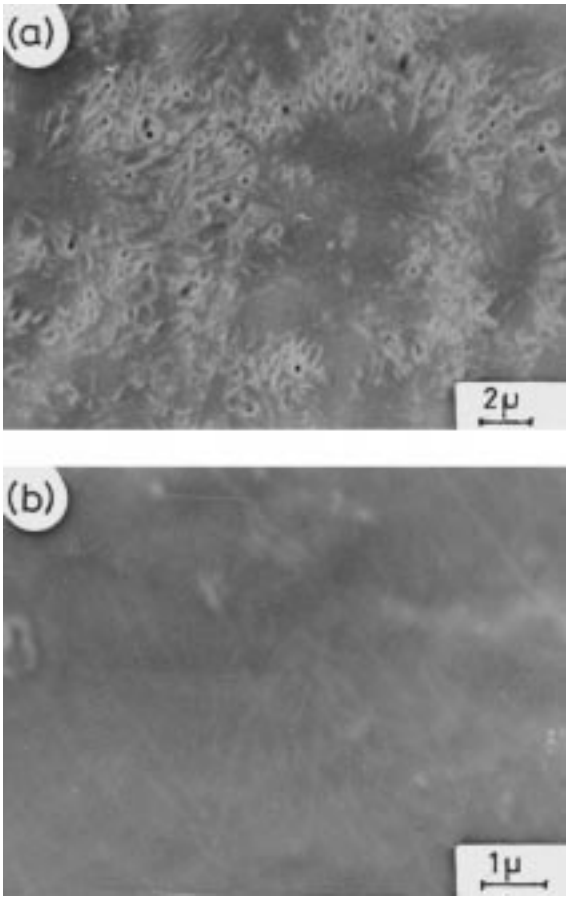

Fig. 9. Scanning electron micrographs of F: (a) a few crystallites of PEO are visible; and (b) micrograph of sample droplet morphology is not evident in the micrograph.

4. Conclusions

Although macroscopically coherent films are formed by PVA and PEO they are inherently immiscible and therefore incompatible. The presence of PEO appears to induce crystallinity in PVA to a small extent in the blends as indicated by thermal and spectroscopic studies. The morphological studies also reveal the ten-

dency towards phase segregation in intermediate blend compositions.

Acknowledgements

The authors wish to thank Professor Manas Chanda for helpful discussion and the referee for very useful comments and suggestions.

References

[1] Pearce EM, Kwei TK, Min BY. J Macromol Sci Chem 1984;A21(89):1181.
[2] Coleman MM, Painter PC. Prog Polym Sci 1995;20:1.
[3] Lee JH, Lee HB, Andrade JD. Prog Polym Sci 1995;20:1043.
[4] Coleman MM, Skrovanek DJ, Hu J, Painter PC. Macromolecules 1988;21:59.
[5] Robsen LM, Hale WF, Merriam CN. Macromolecules 1981;14:1644.
[6] Ting SP, Bulkin BJ, Pearce EM. J Polym Sci: Polym Chem Edn 1981;19:1451.
[7] Cesteros DC, Isasi JR, Katime I. J Polym Sci: Part B: Polym Phys 1994;32:223.
[8] Vinson JA, Vinson JSF, Kingsbury CA. Talanta 1966;19:1673.
[9] Velden GV, Beulen J. Macromolecules 1982;15:1071.
[10] Wu TK, Sheer ML. Macromolecules 1977;10:529.
[11] Bandrup J, Immergut EH. Polymer Handbook. Part VI, 2nd ed. New York, 1975. p. 15.
[12] Stainer M, Charles L, Whitmore DH, Shriver DF. J Electrochem Sci Technol 1984;131:784.
[13] Arnada P, Ruiz-Hitzky E. Chem Mater 1992;4:1395.
[14] Maurya KK, Srivastva N, Hashmi SA, Chandra S. J Mater Sci 1992;27:6357.
[15] Wieczorek W, Such K, Florjanczyk Z, Stevens JR. J Phys Chem 1994;98:6840.
[16] Tubbs RK. J Polym Sci: Part A 1965;3:4181.
[17] Gillham JK, Schwenker RF, Jr. Applied Polymer Symposium 1996;59.
[18] Cobler JG, Haslam J, Willis HA. editors. Identification and Analysis of Polymer, 2nd ed. London: Heyden, 1972. p. 1639 [Chapter 58 "Plastics"].
[19] Wunderlich B. Thermochim Acta 1992;212:131.
[20] Tsuchiya Y, Sumi K. J Polym Sci Part A-1 1969;7:3151.
[21] Cardens G, Munoz C, Tagle LH. J Thermal Anal 1995;44:123.
[22] Madorsky SL, Straus S. J Polym Sci 1959;36:183.
[23] Freeman ES, Carroll B. J Phys Chem 1958;62:394.
[24] Liang CY, Pearson FG. J Polym Sci 1959;35:303.
[25] Papke BL, Ratner MA, Shriver DF. Phys Chem Solids 1981;42:493.
[26] Li X, Hsu SL. J Polym Sci Polym Phys Edn 1984;22:1331.
[27] Satyanarayana DN. Vibrational spectroscopy theory and applications. New Age, 1996. p. 227.
[28] Liu KJ. Macromolecules 1968;1:308.
[29] Scott CE, Macoscko CW. Polymer 1995;36:461.
[30] Bu W, He J. J Appl Polym Sci 1996;62:1445.
[31] Kalfoglou NK, Sotiropoulou DD, Margaritis AG. Eur Polym J 1988;24:389.